

A CONSTRAINED CONVEX SPLITTING SCHEME FOR THE VECTOR-VALUED CAHN–HILLIARD EQUATION

HYUN GEUN LEE¹, JUNE-YUB LEE^{2†}, AND JAEMIN SHIN³

¹DEPARTMENT OF MATHEMATICS, KWANGWOON UNIVERSITY, SEOUL 01897, KOREA
E-mail address: leeh1@kw.ac.kr

²DEPARTMENT OF MATHEMATICS, EWHA WOMANS UNIVERSITY, SEOUL 03760, KOREA
E-mail address: jy1lee@ewha.ac.kr

³INSTITUTE OF MATHEMATICAL SCIENCES, EWHA WOMANS UNIVERSITY, SEOUL 03760, KOREA
E-mail address: jmshin@ewha.ac.kr

ABSTRACT. In contrast to the well-developed convex splitting schemes for gradient flows of two-component system, there were few efforts on applying the convex splitting idea to gradient flows of multi-component system, such as the vector-valued Cahn–Hilliard (vCH) equation. In the case of the vCH equation, one need to consider not only the convex splitting idea but also a specific method to manage the partition of unity constraint to design an unconditionally energy stable scheme. In this paper, we propose a constrained Convex Splitting (cCS) scheme for the vCH equation, which is based on a convex splitting of the energy functional for the vCH equation under the constraint. We show analytically that the cCS scheme is mass conserving and unconditionally uniquely solvable. And it satisfies the constraint at the next time level for any time step thus is unconditionally energy stable. Numerical experiments are presented demonstrating the accuracy, energy stability, and efficiency of the proposed cCS scheme.

1. INTRODUCTION

The Cahn–Hilliard (CH) equation was originally introduced as a phenomenological model of phase separation in a binary alloy [8] and has been applied to a wide range of problems [9]. The CH equation is derived from the Ginzburg–Landau (GL) energy functional:

$$E(c) := \int_{\Omega} \left(F(c) + \frac{\epsilon^2}{2} |\nabla c|^2 \right) dx, \quad (1.1)$$

Received by the editors January 10 2019; Accepted March 19 2019; Published online March 20 2019.

1991 *Mathematics Subject Classification.* 35Q99, 65M70.

Key words and phrases. Vector-valued Cahn–Hilliard equation, Constrained convex splitting, Unconditional unique solvability, Unconditional energy stability.

[†] Corresponding author.

This research was supported by Basic Science Research Program through the National Research Foundation (NRF) funded by the Korea government MSIP(2017R1D1A1B0-3032422,-3034619, 2017R1E1A1A0-3070161).

where Ω is a domain in \mathbb{R}^d ($d = 1, 2, 3$), c is the concentration field, $F(c)$ is the free energy density for c , and $\epsilon > 0$ is the gradient energy coefficient. The CH equation is a gradient flow for the GL energy functional (1.1) in the H^{-1} inner product thus the GL energy functional is nonincreasing in time. Since the CH equation cannot be solved analytically in general, numerical methods are commonly used to study the dynamics of the CH equation. Among them, the convex splitting idea [2, 13, 14] has attracted considerable attention, in which the GL energy functional is split into convex and concave parts:

$$E(c) = E_c(c) - E_e(c) = \int_{\Omega} \left(F_c(c) + \frac{\epsilon^2}{2} |\nabla c|^2 \right) dx - \int_{\Omega} F_e(c) dx,$$

where $F_c(c)$ and $-F_e(c)$ are convex and concave parts of $F(c)$, respectively. And $E_c(c)$ and $E_e(c)$ are treated implicitly and explicitly, respectively. This idea has been applied to develop uniquely solvable and unconditionally energy stable schemes for a wide class of gradient flows [17, 24, 28, 29, 30, 36, 37, 38].

In order to model phase separation in multi-component systems, several generalizations of the GL energy functional have been introduced and studied [5, 6, 7, 10, 11, 12, 15, 16, 18, 19, 20, 21, 22, 23, 25, 26, 27, 31, 32, 33, 34, 35]. However, there were few efforts on applying the convex splitting idea to multi-component systems. There are two noteworthy related works [21, 32]. In [21], a semi-implicit scheme partially using the convex splitting idea was presented to solve multi-component systems. The semi-implicit scheme in [32] treats all the nonlinear term of multi-component systems explicitly and adds an extra stabilizing term. It can be considered as applying the convex splitting idea when the magnitude of the extra stabilizing term is sufficiently large thus the energy stability depends on the magnitude of the extra stabilizing term.

Unlike the CH equation, designing an unconditionally energy stable scheme for multi-component systems requires not only the convex splitting idea but also a specific method to manage the partition of unity constraint (the sum of concentration fields must be unity). Note that the importance of the constraint becomes obvious in proving theorem 3.6 in section 3 and some of numerical schemes add the constraint as a part of explicit equations to be solved not as a consequence of the numerical scheme. The authors in [21] solved multi-component systems only for c_1, \dots, c_{N-1} , where c_i is the concentration field of the phase i and N is the number of

phases, and enforced $c_N = 1 - \sum_{i=1}^{N-1} c_i$ to satisfy the constraint at the next time level. The author in [32] used the Schur complement method to solve multi-component systems for c_1, \dots, c_{N-1} and the constraint $c_1 + \dots + c_N = 1$ together.

In this paper, we propose a constrained Convex Splitting (cCS) scheme for the multi-component system used in [5, 10, 12, 18, 19, 20, 21, 22, 23, 27, 31, 32, 33, 34], referred to as the vector-valued Cahn–Hilliard (vCH) equation. This scheme is based on a convex splitting of the energy functional for the vCH equation under the constraint. We show analytically that the cCS scheme is mass conserving and unconditionally uniquely solvable. And it satisfies the constraint at the next time level for any time step thus is unconditionally energy stable. The

proposed cCS scheme is a first attempt to achieve unconditional energy stability by applying the convex splitting idea to multi-component systems.

This paper is organized as follows. In Section 2, we briefly review the vCH equation. We propose the cCS scheme for the vCH equation in Section 3. In Sections 4 and 5, we present numerical experiments with various free energies. Finally, conclusions are drawn in Section 6.

2. VECTOR-VALUED CAHN–HILLIARD EQUATION

Let $\mathbf{c} = (c_1, \dots, c_N)^T$ be the vector-valued concentration field. Clearly the concentration fields satisfy the partition of unity constraint,

$$c_1 + \dots + c_N = 1. \quad (2.1)$$

Hence admissible states belong to Gibbs N -simplex $G := \left\{ \mathbf{c} \in \mathbb{R}^N \mid \sum_{i=1}^N c_i = 1, 0 \leq c_i \leq 1 \right\}$.

There are several generalizations of the GL energy functional (1.1) to multi-component systems. In this paper, we adopt the approach used in [5, 10, 12, 18, 19, 20, 21, 22, 23, 27, 31, 32, 33, 34], where the energy functional is defined as follows:

$$\mathcal{E}(\mathbf{c}) := \int_{\Omega} \left(\mathcal{F}(\mathbf{c}) + \frac{\epsilon^2}{2} \sum_{i=1}^N |\nabla c_i|^2 \right) d\mathbf{x}, \quad (2.2)$$

referred to as the vGL the energy functional. There are two typical choices for $\mathcal{F}(\mathbf{c})$: the polynomial free energy [20, 21, 22, 23, 27, 31, 32, 33, 34]

$$\mathcal{F}(\mathbf{c}) = \frac{1}{4} \sum_{i=1}^N c_i^2 (c_i - 1)^2$$

and logarithmic free energy [5, 10, 12, 18, 19, 32]

$$\mathcal{F}(\mathbf{c}) = \theta \sum_{i=1}^N c_i \ln c_i + \theta_c \sum_{i=1}^N \sum_{j=i+1}^N c_i c_j = \theta \sum_{i=1}^N c_i \ln c_i + \frac{\theta_c}{2} \sum_{i=1}^N c_i (1 - c_i),$$

where θ and θ_c are the absolute and critical temperatures, respectively. The vCH equation is a gradient flow for the vGL energy functional (2.2) in the H^{-1} inner product under the constraint (2.1). In order to ensure (2.1), we use a Lagrange multiplier $\alpha(\mathbf{c})$ [6, 16, 18, 19, 21, 22, 23, 26, 35]. Then, the vCH equation becomes

$$\begin{aligned} \frac{\partial \mathbf{c}}{\partial t} &= \Delta \boldsymbol{\mu}, \quad \boldsymbol{\mu} := \frac{\delta \mathcal{E}}{\delta \mathbf{c}} = \mathbf{f}(\mathbf{c}) - \epsilon^2 \Delta \mathbf{c} + \alpha(\mathbf{c}) \mathbf{1}, \quad \mathbf{x} \in \Omega, \quad 0 < t \leq T, \\ c_i(\mathbf{x}, 0) &= c_i^0(\mathbf{x}), \quad \nabla c_i \cdot \mathbf{n} = \nabla \mu_i \cdot \mathbf{n} = 0 \quad \text{on } \partial\Omega, \quad \text{for } i = 1, \dots, N, \end{aligned} \quad (2.3)$$

where $\boldsymbol{\mu} = (\mu_1, \dots, \mu_N)^T$ is the vector-valued chemical potential, μ_i is the chemical potential of the phase i , $\frac{\delta}{\delta \mathbf{c}}$ denotes the variational derivative with respect to \mathbf{c} , $\mathbf{f}(\mathbf{c}) = \frac{\partial \mathcal{F}}{\partial \mathbf{c}} =$

$\left(\frac{\partial \mathcal{F}}{\partial c_1}, \dots, \frac{\partial \mathcal{F}}{\partial c_N}\right)^T = (f(c_1), \dots, f(c_N))^T$, $\mathbf{1} = (1, \dots, 1)^T \in \mathbb{R}^N$, \mathbf{n} is a unit normal vector to $\partial\Omega$, and

$$\alpha(\mathbf{c}) = -\frac{1}{N} \sum_{i=1}^N f(c_i).$$

Because the vCH equation (2.3) is of gradient type, the vGL energy functional is nonincreasing in time as the partition of unity constraint holds:

$$\begin{aligned} \frac{d\mathcal{E}}{dt} &= \int_{\Omega} \sum_{i=1}^N \left(\frac{\partial \mathcal{F}}{\partial c_i} \frac{\partial c_i}{\partial t} + \epsilon^2 \nabla c_i \cdot \nabla \frac{\partial c_i}{\partial t} \right) d\mathbf{x} = \int_{\Omega} \sum_{i=1}^N (f(c_i) - \epsilon^2 \Delta c_i) \frac{\partial c_i}{\partial t} d\mathbf{x} \\ &= \int_{\Omega} \sum_{i=1}^N (\mu_i - \alpha(\mathbf{c})) \frac{\partial c_i}{\partial t} d\mathbf{x} = \int_{\Omega} \sum_{i=1}^N \mu_i \Delta \mu_i d\mathbf{x} - \int_{\Omega} \alpha(\mathbf{c}) \frac{\partial}{\partial t} \sum_{i=1}^N c_i d\mathbf{x} \\ &= - \int_{\Omega} \sum_{i=1}^N |\nabla \mu_i|^2 d\mathbf{x} \leq 0. \end{aligned}$$

3. CONSTRAINED CONVEX SPLITTING SCHEME FOR THE VECTOR-VALUED CAHN–HILLIARD EQUATION

In this section, we propose an unconditionally energy stable scheme for the vCH equation (2.3). The scheme is based on the observation that the vGL energy functional (2.2) can be split into convex and concave parts:

$$\mathcal{E}(\mathbf{c}) = \mathcal{E}_c(\mathbf{c}) - \mathcal{E}_e(\mathbf{c}) = \int_{\Omega} \left(\mathcal{F}_c(\mathbf{c}) + \frac{\epsilon^2}{2} \sum_{i=1}^N |\nabla c_i|^2 \right) d\mathbf{x} - \int_{\Omega} \mathcal{F}_e(\mathbf{c}) d\mathbf{x},$$

where $\mathcal{F}_c(\mathbf{c})$ and $-\mathcal{F}_e(\mathbf{c})$ are convex and concave parts of $\mathcal{F}(\mathbf{c})$, respectively. Treating $\mathcal{E}_c(\mathbf{c})$ implicitly and $\mathcal{E}_e(\mathbf{c})$ explicitly, the constrained Convex Splitting (cCS) scheme is obtained:

$$\frac{\mathbf{c}^{n+1} - \mathbf{c}^n}{\Delta t} = \Delta \boldsymbol{\mu}^{n+1}, \quad (3.1)$$

$$\begin{aligned} \boldsymbol{\mu}^{n+1} &:= \frac{\delta \mathcal{E}_c(\mathbf{c}^{n+1})}{\delta \mathbf{c}} - \frac{\delta \mathcal{E}_e(\mathbf{c}^n)}{\delta \mathbf{c}} \\ &= \mathbf{f}_c(\mathbf{c}^{n+1}) - \epsilon^2 \Delta \mathbf{c}^{n+1} + \alpha_c(\mathbf{c}^{n+1}) \mathbf{1} - \mathbf{f}_e(\mathbf{c}^n) - \alpha_e(\mathbf{c}^n) \mathbf{1}, \end{aligned} \quad (3.2)$$

where $\mathbf{f}_c(\mathbf{c}) = \frac{\partial \mathcal{F}_c}{\partial \mathbf{c}} = (f_c(c_1), \dots, f_c(c_N))^T$, $\mathbf{f}_e(\mathbf{c}) = \frac{\partial \mathcal{F}_e}{\partial \mathbf{c}} = (f_e(c_1), \dots, f_e(c_N))^T$,

$$\alpha_c(\mathbf{c}) = -\frac{1}{N} \sum_{i=1}^N f_c(c_i), \quad \text{and} \quad \alpha_e(\mathbf{c}) = -\frac{1}{N} \sum_{i=1}^N f_e(c_i).$$

Remark 3.1. The choices of $\alpha_c(\mathbf{c}^{n+1})$ and $\alpha_e(\mathbf{c}^n)$ in the cCS scheme (3.1) and (3.2) are critical factors to satisfy the partition of unity constraint (2.1) and have the unconditional energy

stability. $\alpha_c(\mathbf{c}^{n+1})$ and $\alpha_e(\mathbf{c}^n)$ are obtained by taking the variational derivative of $\mathcal{E}_c(\mathbf{c}^{n+1})$ and $\mathcal{E}_e(\mathbf{c}^n)$ with respect to \mathbf{c} under the constraints $\sum_{i=1}^N c_i^{n+1} = 1$ and $\sum_{i=1}^N c_i^n = 1$, respectively.

Lemma 3.2. *The cCS scheme is mass conserving.*

Proof. Let c_i^{n+1} ($i = 1, \dots, N$) be a solution of the cCS scheme. From Eq. (3.1), we have

$$\frac{1}{\Delta t} \int_{\Omega} (c_i^{n+1} - c_i^n) d\mathbf{x} = \int_{\Omega} \Delta \mu_i^{n+1} d\mathbf{x} = \int_{\partial\Omega} \nabla \mu_i^{n+1} \cdot \mathbf{n} ds = 0, \quad \text{for } i = 1, \dots, N,$$

where we used the zero Neumann boundary condition for μ_i^{n+1} . It follows that $\int_{\Omega} c_i^{n+1} d\mathbf{x} = \int_{\Omega} c_i^n d\mathbf{x}$ for each i . \square

Lemma 3.3. *The cCS scheme satisfies the constraint (2.1) at any time t^n , i.e., $\sum_{i=1}^N c_i^n = 1$ if an initial condition satisfies $\sum_{i=1}^N c_i^0 = 1$.*

Proof. Since $\sum_{i=1}^N f_c(c_i^{n+1}) + N\alpha_c(\mathbf{c}^{n+1}) = 0$ and $\sum_{i=1}^N f_e(c_i^n) + N\alpha_e(\mathbf{c}^n) = 0$, we have from Eqs. (3.1) and (3.2)

$$\begin{aligned} \frac{1}{\Delta t} \sum_{i=1}^N (c_i^{n+1} - c_i^n) &= -\epsilon^2 \Delta^2 \sum_{i=1}^N c_i^{n+1}, \\ \text{i.e., } (\mathcal{I} + \Delta t \epsilon^2 \Delta^2) \sum_{i=1}^N c_i^{n+1} &= \sum_{i=1}^N c_i^n, \end{aligned} \quad (3.3)$$

where \mathcal{I} denotes the identity operator. Since $\mathcal{I} + \Delta t \epsilon^2 \Delta^2$ with a zero Neumann boundary condition for c_i is an invertible operator, Eq. (3.3) has a unique solution. Thus, Eq. (3.3) ensures that $\sum_{i=1}^N c_i^{n+1} = 1$ for all $n \geq 0$ with the initial condition satisfying $\sum_{i=1}^N c_i^0 = 1$. \square

Theorem 3.4. *The cCS scheme is uniquely solvable for any time step $\Delta t > 0$.*

Proof. We consider the following functional on $\tilde{H} = \left\{ \mathbf{c} \mid \sum_{i=1}^N c_i = 1, \int_{\Omega} c_i \, d\mathbf{x} = \int_{\Omega} c_i^n \, d\mathbf{x} \right.$
for $i = 1, \dots, N \left. \right\}$:

$$G(\mathbf{c}) = \frac{1}{2\Delta t} \|\mathbf{c} - \mathbf{c}^n\|_{H^{-1}}^2 + \mathcal{E}_c(\mathbf{c}) - \left(\frac{\delta \mathcal{E}_e(\mathbf{c}^n)}{\delta \mathbf{c}}, \mathbf{c} \right)_{L^2},$$

where $(\mathbf{c}, \mathbf{d})_{L^2} = \int_{\Omega} \mathbf{c} \cdot \mathbf{d} \, d\mathbf{x} = \int_{\Omega} \sum_{i=1}^N c_i d_i \, d\mathbf{x}$.

It may be shown that $\mathbf{c}^{n+1} \in \tilde{H}$ is the unique minimizer of $G(\mathbf{c})$ if and only if it solves,

for any $\mathbf{d} \in H_0 = \left\{ \mathbf{d} \mid \sum_{i=1}^N d_i = 0, \int_{\Omega} d_i \, d\mathbf{x} = 0 \text{ for } i = 1, \dots, N \right\}$,

$$\left. \frac{dG(\mathbf{c} + s\mathbf{d})}{ds} \right|_{s=0} = \left(\frac{\mathbf{c} - \mathbf{c}^n}{\Delta t}, \mathbf{d} \right)_{H^{-1}} + \left(\frac{\delta \mathcal{E}_c(\mathbf{c})}{\delta \mathbf{c}} - \frac{\delta \mathcal{E}_e(\mathbf{c}^n)}{\delta \mathbf{c}}, \mathbf{d} \right)_{L^2} \quad (3.4)$$

$$= \left(\frac{\mathbf{c} - \mathbf{c}^n}{\Delta t} - \Delta \left(\frac{\delta \mathcal{E}_c(\mathbf{c})}{\delta \mathbf{c}} - \frac{\delta \mathcal{E}_e(\mathbf{c}^n)}{\delta \mathbf{c}} \right), \mathbf{d} \right)_{H^{-1}} = 0, \quad (3.5)$$

because $G(\mathbf{c})$ is strictly convex by

$$\left. \frac{d^2 G(\mathbf{c} + s\mathbf{d})}{ds^2} \right|_{s=0} = \frac{1}{\Delta t} \|\mathbf{d}\|_{H^{-1}}^2 + \int_{\Omega} \sum_{i=1}^N \left(f'_c(c_i) d_i^2 + \epsilon^2 |\nabla d_i|^2 \right) d\mathbf{x} \geq 0.$$

Here, the second term on the right-hand side of Eq. (3.4) is obtained as follows:

$$\begin{aligned} & \left. \frac{d}{ds} \int_{\Omega} \left(\mathcal{F}_c(\mathbf{c} + s\mathbf{d}) + \frac{\epsilon^2}{2} \sum_{i=1}^N |\nabla(c_i + s d_i)|^2 \right) d\mathbf{x} \right|_{s=0} \\ &= \int_{\Omega} \left(\mathbf{f}_c(\mathbf{c}) \cdot \mathbf{d} + \epsilon^2 \sum_{i=1}^N \nabla c_i \cdot \nabla d_i \right) d\mathbf{x} = \int_{\Omega} \left(\mathbf{f}_c(\mathbf{c}) - \epsilon^2 \Delta \mathbf{c} \right) \cdot \mathbf{d} \, d\mathbf{x} \\ &= \int_{\Omega} \left(\mathbf{f}_c(\mathbf{c}) - \epsilon^2 \Delta \mathbf{c} + \alpha_c(\mathbf{c}) \mathbf{1} \right) \cdot \mathbf{d} \, d\mathbf{x} - \int_{\Omega} \alpha_c(\mathbf{c}) \mathbf{1} \cdot \mathbf{d} \, d\mathbf{x} = \left(\frac{\delta \mathcal{E}_c(\mathbf{c})}{\delta \mathbf{c}}, \mathbf{d} \right)_{L^2}. \end{aligned}$$

And, Eq. (3.5) is true for any $\mathbf{d} \in H_0$ if and only if the given equation holds

$$\frac{\mathbf{c}^{n+1} - \mathbf{c}^n}{\Delta t} = \Delta \left(\frac{\delta \mathcal{E}_c(\mathbf{c}^{n+1})}{\delta \mathbf{c}} - \frac{\delta \mathcal{E}_e(\mathbf{c}^n)}{\delta \mathbf{c}} \right).$$

Hence, minimizing the strictly convex functional $G(\mathbf{c})$ is equivalent to solving Eqs. (3.1) and (3.2). \square

Lemma 3.5. Consider the following convex splitting of the GL energy functional (1.1):

$$E(c) = E_c(c) - E_e(c) = \int_{\Omega} \left(F_c(c) + \frac{\epsilon^2}{2} |\nabla c|^2 \right) d\mathbf{x} - \int_{\Omega} F_e(c) d\mathbf{x}, \text{ where } F'_c(c) = f_c(c) \text{ and } F'_e(c) = f_e(c). \text{ Then, the convexity of } E_c(c) \text{ and } E_e(c) \text{ yields the following inequality:}$$

$$\begin{aligned} E(c^{n+1}) - E(c^n) &\leq \int_{\Omega} \left(\frac{\delta E_c(c^{n+1})}{\delta c} - \frac{\delta E_e(c^n)}{\delta c} \right) (c^{n+1} - c^n) d\mathbf{x} \\ &= \int_{\Omega} \left(f_c(c^{n+1}) - \epsilon^2 \Delta c^{n+1} - f_e(c^n) \right) (c^{n+1} - c^n) d\mathbf{x}. \end{aligned}$$

Proof. We refer to [37]. □

Theorem 3.6. The cCS scheme with an initial condition satisfying $\sum_{i=1}^N c_i^0 = 1$ is unconditionally energy stable, meaning that for any $\Delta t > 0$,

$$\mathcal{E}(\mathbf{c}^{n+1}) \leq \mathcal{E}(\mathbf{c}^n).$$

Proof. Using Lemma 3.5, we have

$$\begin{aligned} \mathcal{E}(\mathbf{c}^{n+1}) - \mathcal{E}(\mathbf{c}^n) &= \sum_{i=1}^N \left(E(c_i^{n+1}) - E(c_i^n) \right) \\ &\leq \sum_{i=1}^N \int_{\Omega} \left(f_c(c_i^{n+1}) - \epsilon^2 \Delta c_i^{n+1} - f_e(c_i^n) \right) (c_i^{n+1} - c_i^n) d\mathbf{x}. \end{aligned}$$

And we obtain from Lemma 3.3

$$\begin{aligned} \mathcal{E}(\mathbf{c}^{n+1}) - \mathcal{E}(\mathbf{c}^n) &\leq \sum_{i=1}^N \int_{\Omega} \left(\mu_i^{n+1} - \alpha_c(\mathbf{c}^{n+1}) + \alpha_e(\mathbf{c}^n) \right) (c_i^{n+1} - c_i^n) d\mathbf{x} \\ &= \Delta t \sum_{i=1}^N \int_{\Omega} \mu_i^{n+1} \Delta \mu_i^{n+1} d\mathbf{x} \\ &\quad - \int_{\Omega} \left(\alpha_c(\mathbf{c}^{n+1}) - \alpha_e(\mathbf{c}^n) \right) \sum_{i=1}^N (c_i^{n+1} - c_i^n) d\mathbf{x} \\ &= -\Delta t \sum_{i=1}^N \int_{\Omega} |\nabla \mu_i^{n+1}|^2 d\mathbf{x} \leq 0. \end{aligned}$$

□

4. NUMERICAL EXPERIMENTS WITH THE POLYNOMIAL FREE ENERGY

For numerical tests, we consider the polynomial free energy $\mathcal{F}(\mathbf{c}) = \frac{1}{4} \sum_{i=1}^N c_i^2 (c_i - 1)^2$ and following splitting:

$$\mathcal{F}_c(\mathbf{c}) = \frac{1}{4} \sum_{i=1}^N c_i^2, \quad \mathcal{F}_e(\mathbf{c}) = \sum_{i=1}^N \Psi(c_i), \quad \Psi(c) := \begin{cases} 0, & c < 0 \\ \frac{1}{4}(2c^3 - c^4), & c \in [0, 1] \\ \frac{1}{4}(-1 + 2c), & c > 1 \end{cases} \quad (4.1)$$

to have both convexity of $\mathcal{F}_c(\mathbf{c})$ and $\mathcal{F}_e(\mathbf{c})$ for the extended range of \mathbf{c} and easiness of implementation. Then, $f_c(c) = \frac{1}{2}c$ and $f_e(c) = \Psi'(c)$, and the cCS scheme with $\mathcal{F}_c(\mathbf{c})$ and $\mathcal{F}_e(\mathbf{c})$ in (4.1) becomes

$$\frac{\mathbf{c}^{n+1} - \mathbf{c}^n}{\Delta t} = \Delta \left(\frac{1}{2} \mathbf{c}^{n+1} - \epsilon^2 \Delta \mathbf{c}^{n+1} - \frac{1}{2N} \sum_{i=1}^N c_i^{n+1} \mathbf{1} - \mathbf{f}_c(\mathbf{c}^n) - \alpha_e(\mathbf{c}^n) \mathbf{1} \right). \quad (4.2)$$

By Lemma 3.3, Eq. (4.2) can be rewritten as follows:

$$\frac{\mathbf{c}^{n+1} - \mathbf{c}^n}{\Delta t} = \Delta \left(\frac{1}{2} \mathbf{c}^{n+1} - \epsilon^2 \Delta \mathbf{c}^{n+1} - \mathbf{f}_c(\mathbf{c}^n) - \alpha_e(\mathbf{c}^n) \mathbf{1} \right).$$

Since $\mathbf{f}_c(\mathbf{c})$ is linear with respect to \mathbf{c} , the scheme allows to solve the vCH equation componentwisely,

$$\mathcal{D} c_i^{n+1} = b_i^n, \quad \text{i.e.,} \quad c_i^{n+1} = \mathcal{D}^{-1} b_i^n, \quad \text{for } i = 1, \dots, N,$$

where $\mathcal{D} := \mathcal{I} - \Delta t \Delta (\frac{1}{2} - \epsilon^2 \Delta)$ is invertible with a zero Neumann boundary condition for c_i and $b_i^n := c_i^n - \Delta t \Delta (f_e(c_i^n) + \alpha_e(\mathbf{c}^n))$ is given explicitly.

We here use the Fourier spectral method for the spatial discretization and the discrete cosine transform in MATLAB is applied for the whole numerical simulations to solve the vCH equation with the zero Neumann boundary condition.

4.1. Convergence test. We demonstrate the convergence of the proposed scheme with the initial conditions

$$\begin{aligned} c_1(x, 0) &= \frac{1}{3} + 0.01 \cos \frac{3}{2}x, & c_2(x, 0) &= \frac{1}{3} + 0.02 \cos x, \\ c_3(x, 0) &= 1 - c_1(x, 0) - c_2(x, 0) \end{aligned}$$

on $\Omega = [0, 2\pi]$. We set $\epsilon = 0.25$ and compute $\mathbf{c}(x, t)$ for $0 < t \leq 280$. The grid size is fixed to $h = 2\pi/128$ which provides enough spatial accuracy. In order to estimate the convergence rate with respect to Δt , simulations are performed by varying $\Delta t = 2^{-10}, 2^{-9}, \dots, 2^2$. We take the quadruply over-resolved numerical solution as the reference solution. Figures 1 (a) and (b) show the evolution of $\mathcal{E}(t)$ for the reference solution and the relative l_2 -errors of $\mathbf{c}(x, 120)$ (this time is indicated by a dashed line in Fig. 1 (a)) for various time steps, respectively. It is observed that the scheme is first-order accurate in time.

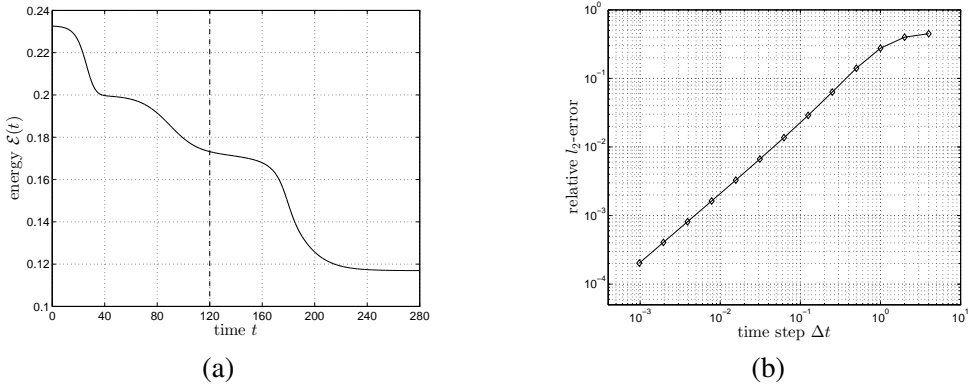


FIGURE 1. (a) Evolution of $\mathcal{E}(t)$ for the reference solution with $\epsilon = 0.25$ and $h = 2\pi/128$. (b) Relative l_2 -errors of $\mathbf{c}(x, 120)$ for various time steps.

4.2. Energy stability of the proposed scheme. In order to investigate the energy stability of the proposed scheme, we consider the phase separation of a ternary system with the initial conditions

$$\begin{aligned} c_1(x, y, 0) &= \frac{1}{3} + \text{rand}(x, y), & c_2(x, y, 0) &= \frac{1}{3} + \text{rand}(x, y), \\ c_3(x, y, 0) &= 1 - c_1(x, y, 0) - c_2(x, y, 0) \end{aligned}$$

on $\Omega = [0, 2\pi] \times [0, 2\pi]$. Here, $\text{rand}(x, y)$ is a random number between -0.1 and 0.1 , and we use $\epsilon = 0.1$ and $h = 2\pi/128$.

Figure 2 shows the evolution of $\mathcal{E}(t)$ using the explicit Euler's and the proposed scheme with different time steps. The energy curves for the explicit Euler scheme with $\Delta t = 2^{-20}$ and 2^{-19} are nonincreasing until $t = 2^{-14}$, whereas the energy curve with $\Delta t = 2^{-18}$ increases rapidly after $t = 2^{-16}$. As we can see this figure, the explicit Euler's scheme has a severe time step restriction for energy stability. All the energy curves using the proposed scheme are nonincreasing in time even for sufficiently large time steps. Figure 3 shows the evolution of $\mathbf{c}(x, y, t)$ with $\Delta t = 2^{-10}$.

4.3. Efficiency of the proposed scheme. In order to show the efficiency of the proposed scheme, we consider the phase separation of $3, \dots, 10$ components ($N = 3, \dots, 10$). For each N , the initial conditions are chosen as follows: the domain $\Omega = [0, 2\pi] \times [0, 2\pi]$ is partitioned into 40 Voronoi cells and c_i is set to 1 on randomly selected Voronoi cells for $i = 1, \dots, N$. $\epsilon = 0.05$, $h = 2\pi/128$, and $\Delta t = 1/4$ are used. Simulations are run until $T = 512$ and Fig. 4 shows the evolution of $\mathbf{c}(x, y, t)$ at $t = 0$ and 512. Figure 5 presents the CPU time (in seconds, averaged over 10 trials performed on Intel Core i5-7500 CPU at 3.40GHz with 8GB RAM) consumed for $N = 3, \dots, 10$. The results suggest that the CPU time is almost linear with respect to the number of components N .

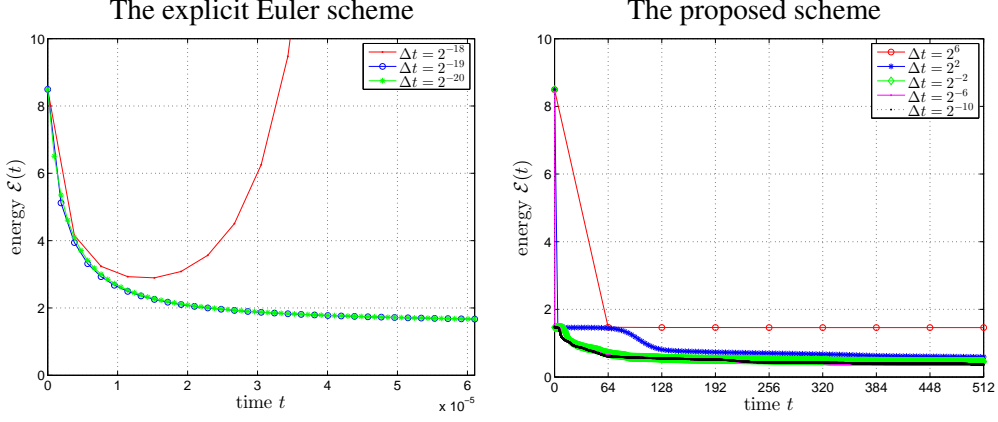


FIGURE 2. Evolution of $\mathcal{E}(t)$ using the explicit Euler's and the proposed scheme with different time steps.

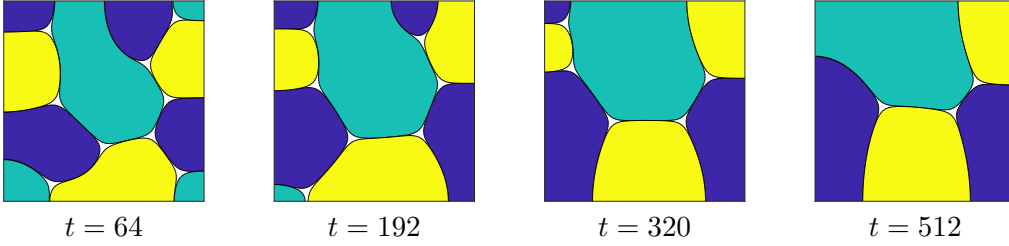


FIGURE 3. Evolution of $\mathbf{c}(x, y, t)$ with $\epsilon = 0.1$, $h = 2\pi/128$, and $\Delta t = 2^{-10}$. In each snapshots, the yellow, green, and blue regions indicate c_1 , c_2 , and c_3 , respectively, and contour lines represent $c_i = 0.5$.

4.4. Phase separation of a four-component mixture in 3D. We solve the vCH equation on $\Omega = [0, 2\pi] \times [0, 2\pi] \times [0, 2\pi]$ with $\epsilon = 0.1$, $h = 2\pi/64$, and $\Delta t = 1/4$. The initial conditions are

$$c_i(x, y, z, 0) = \frac{1}{4} + i \cdot \text{rand}(x, y, z), \quad \text{for } i = 1, 2, 3,$$

$$c_4(x, y, z, 0) = 1 - \sum_{i=1}^3 c_i(x, y, z, 0),$$

where $\text{rand}(x, y, z)$ is a random number between -0.01 and 0.01 at the grid points. Figures 6 and 7 show the evolution of $\mathbf{c}(x, y, z, t)$ and its energy, respectively. We observe that the randomly perturbed constant concentration fields evolve to many small structures and then to single-interface structures as the energy is dissipated in time.

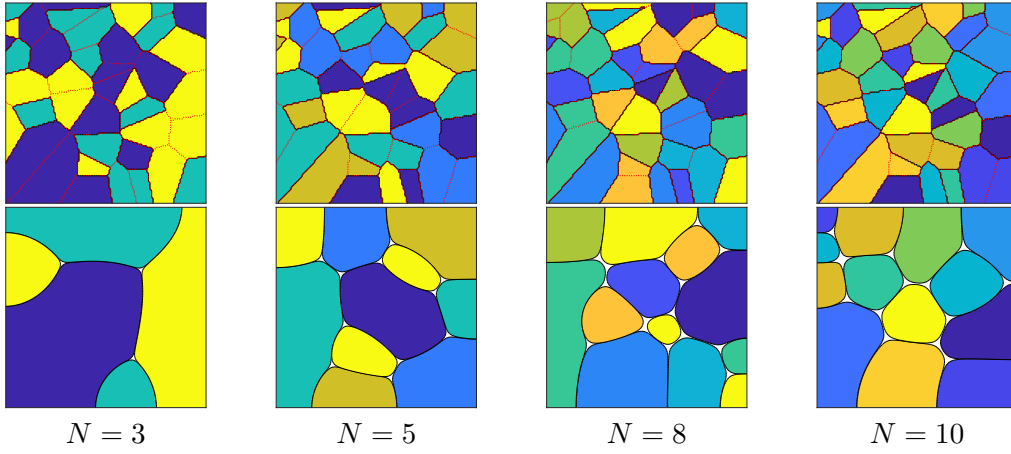


FIGURE 4. Evolution of $c(x, y, t)$ at $t = 0$ (top) and 512 (bottom) with $\epsilon = 0.05$, $h = 2\pi/128$, and $\Delta t = 1/4$. Columns 1–4 correspond to $N = 3, 5, 8$, and 10, respectively. In the top, the 40 Voronoi cells are represented by red dotted lines.

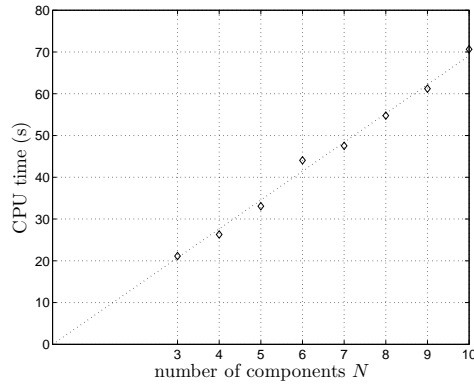


FIGURE 5. CPU time versus the number of components. Each simulation is run until $T = 512$. Each line segment is obtained by least squares fitting of all points.

5. NUMERICAL EXPERIMENTS WITH THE LOGARITHMIC FREE ENERGY

In this section, we consider the logarithmic free energy

$$\mathcal{F}(\mathbf{c}) = \theta \sum_{i=1}^N c_i \ln c_i + \theta_c \sum_{i=1}^N \sum_{j=i+1}^N c_i c_j = \theta \sum_{i=1}^N c_i \ln c_i + \frac{\theta_c}{2} \sum_{i=1}^N c_i (1 - c_i).$$

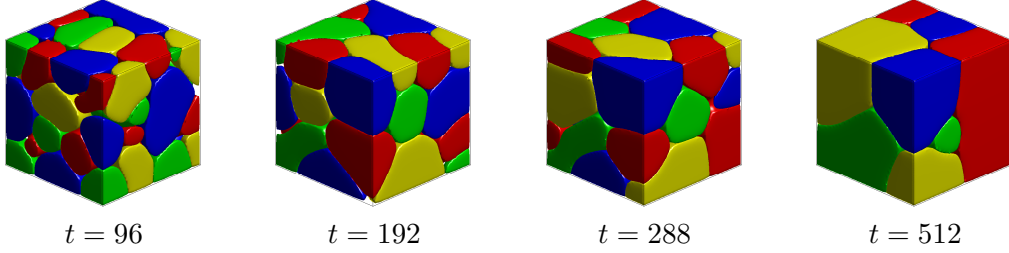


FIGURE 6. Evolution of $\mathbf{c}(x, y, z, t)$ with $\epsilon = 0.1$, $h = 2\pi/64$, and $\Delta t = 1/4$. In each snapshots, the red, green, blue, and yellow regions indicate c_1 , c_2 , c_3 , and c_4 , respectively.

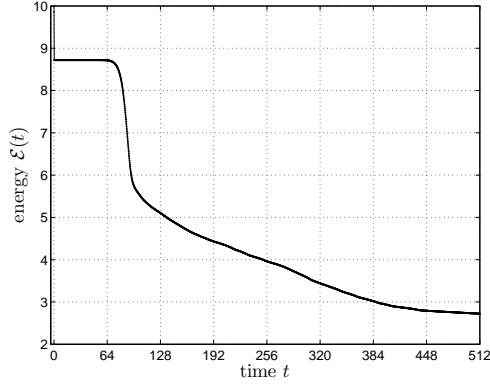


FIGURE 7. Evolution of $\mathcal{E}(t)$.

Unlike the polynomial free energy, a nonlinear convex splitting is a natural choice for the logarithmic free energy:

$$\mathcal{F}_c(\mathbf{c}) = \theta \sum_{i=1}^N c_i \ln c_i, \quad \mathcal{F}_e(\mathbf{c}) = -\frac{\theta_c}{2} \sum_{i=1}^N c_i(1 - c_i).$$

Then, $f_c(c) = \theta \ln c$ and $f_e(c) = \theta_c c$. In the case of the logarithmic free energy, there is a numerical difficulty associated with the singularity as each c_i approaches zero. In order to avoid this, we apply a regularization to the logarithmic function, i.e., for a small positive number δ , we define

$$\ln_\delta c := \begin{cases} \ln c, & \text{if } c \geq \delta, \\ p(c) = -\frac{1}{2\delta^2}c^2 + \frac{2}{\delta}c + \ln \delta - \frac{3}{2}, & \text{otherwise,} \end{cases}$$

where the quadratic polynomial $p(c)$ matches the values of zeroth, first, and second derivatives of the logarithmic function at $c = \delta$ [3, 4].

The nonlinearity of the scheme comes from $f_c(c_i^{n+1})$ and $\alpha_c(\mathbf{c}^{n+1})$ and these can be handled using a Newton-type linearization [24, 28]

$$\begin{aligned} f_c(c_i^{n,m+1}) &\approx f_c(c_i^{n,m}) + f'_c(c_i^{n,m})(c_i^{n,m+1} - c_i^{n,m}), \\ \alpha_c(\mathbf{c}^{n,m+1}) &\approx \alpha_c(\mathbf{c}^{n,m}) + \frac{\partial \alpha_c(\mathbf{c}^{n,m})^T}{\partial \mathbf{c}} (\mathbf{c}^{n,m+1} - \mathbf{c}^{n,m}) \\ &= -\frac{1}{N} \sum_{i=1}^N \left(f_c(c_i^{n,m}) + f'_c(c_i^{n,m})(c_i^{n,m+1} - c_i^{n,m}) \right) \end{aligned}$$

for $m = 0, 1, \dots$. We then develop a Newton-type fixed point iteration method for the cCS scheme as

$$\begin{pmatrix} \mathcal{D}_1 + \mathcal{A}_1 & \mathcal{A}_2 & \cdots & \mathcal{A}_N \\ \mathcal{A}_1 & \mathcal{D}_2 + \mathcal{A}_2 & \cdots & \mathcal{A}_N \\ \vdots & \vdots & \ddots & \vdots \\ \mathcal{A}_1 & \mathcal{A}_2 & \cdots & \mathcal{D}_N + \mathcal{A}_N \end{pmatrix} \begin{pmatrix} c_1^{n,m+1} - c_1^{n,m} \\ c_2^{n,m+1} - c_2^{n,m} \\ \vdots \\ c_N^{n,m+1} - c_N^{n,m} \end{pmatrix} = \begin{pmatrix} b_1^{n,m} \\ b_2^{n,m} \\ \vdots \\ b_N^{n,m} \end{pmatrix}, \quad (5.1)$$

where $\mathbf{c}^{n,0} = \mathbf{c}^n$,

$$\begin{aligned} \mathcal{D}_i &= \mathcal{I} - \Delta t \Delta (f'_c(c_i^{n,m}) - \epsilon^2 \Delta), \quad \mathcal{A}_i = -\Delta t \Delta \left(-\frac{1}{N} f'_c(c_i^{n,m}) \right), \\ b_i^{n,m} &= c_i^n - c_i^{n,m} + \Delta t \Delta (f_c(c_i^{n,m}) - \epsilon^2 \Delta c_i^{n,m} + \alpha_c(\mathbf{c}^{n,m}) - f_c(c_i^n) - \alpha_c(\mathbf{c}^n)), \end{aligned}$$

for $i = 1, \dots, N$, and we set

$$\mathbf{c}^{n+1} = \mathbf{c}^{n,m+1}$$

if a relative l_2 -norm of the consecutive error $\frac{\|\mathbf{c}^{n,m+1} - \mathbf{c}^{n,m}\|_2}{\|\mathbf{c}^{n,m}\|_2}$ is less than a tolerance tol . In this paper, the biconjugate gradient (BICG) method is used to solve the system (5.1) and we use the following preconditioner P to accelerate the convergence speed of the BICG algorithm:

$$P = \begin{pmatrix} \bar{\mathcal{D}}_1 & 0 & \cdots & 0 \\ 0 & \bar{\mathcal{D}}_2 & \cdots & 0 \\ \vdots & \vdots & \ddots & \vdots \\ 0 & 0 & \cdots & \bar{\mathcal{D}}_N \end{pmatrix},$$

where $\bar{\mathcal{D}}_i = \mathcal{I} - \Delta t \Delta (\overline{f'_c(c_i^{n,m})} - \epsilon^2 \Delta)$ and $\overline{f'_c(c_i^{n,m})}$ is the average value of $f'_c(c_i^{n,m})$. The stopping criterion for the BICG iteration is that the relative residual norm is less than tol .

5.1. Robustness of the nonlinear solver and convergence test. In order to show the robustness of the nonlinear solver and the necessity of the preconditioner, we count the number of nonlinear and BICG iterations with the initial conditions

$$\begin{aligned} c_1(x, 0) &= \frac{1}{3} + 0.01 \cos \frac{3}{2}x, \quad c_2(x, 0) = \frac{1}{3} + 0.02 \cos x, \\ c_3(x, 0) &= 1 - c_1(x, 0) - c_2(x, 0) \end{aligned}$$

on $\Omega = [0, 2\pi]$, $\theta = 0.3$, $\theta_c = 1$, $\epsilon = 0.25$, $h = 2\pi/128$, and $tol = 10^{-10}$. Figure 8 shows the number of BICG iterations without and with the preconditioner during the simulation time $0 < t = n\Delta t \leq 280$ for different time steps. As shown in Fig. 8, the BICG iterations were remarkably reduced (about 100 times) by using the preconditioner. Figures 9 (a) and (b)

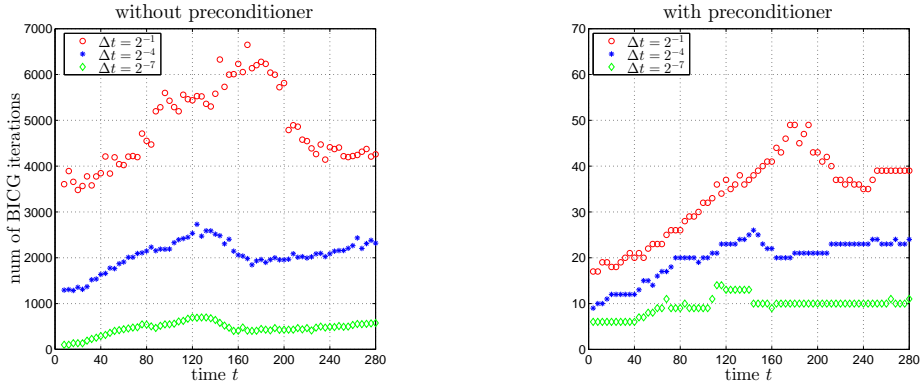


FIGURE 8. Number of BICG iterations without and with the preconditioner for different time steps.

show the number of nonlinear and BICG iterations (with the preconditioner) averaged over the simulation time, respectively. 2–4 nonlinear iterations (on average) were involved in proceeding to the next time level. We believe that such a fast iterative convergence can be achieved since the successive iteration (5.1) is a Newton-type fixed point iteration method. And 6–42 BICG iterations (on average) were involved in proceeding to the next time level owing to the preconditioner.

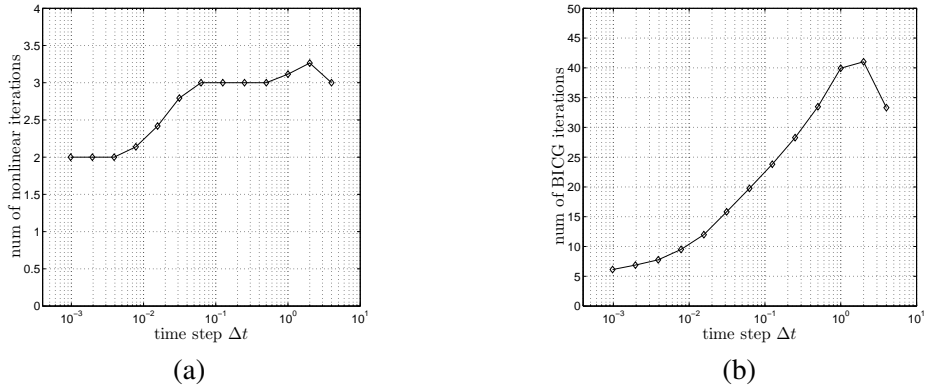


FIGURE 9. Number of (a) nonlinear and (b) BICG iterations (with the preconditioner) averaged over the simulation time.

Next, we vary $\Delta t = 2^{-10}, 2^{-9}, \dots, 2^2$ to estimate the convergence rate with respect to Δt for the logarithmic free energy. We take the quadruply over-resolved numerical solution as the reference solution. Figures 10 (a) and (b) show the evolution of $\mathcal{E}(t)$ for the reference solution and the relative l_2 -errors of $c(x, 120)$ (this time is indicated by a dashed line in Fig. 10 (a)) for various time steps, respectively. It is observed that the scheme is also first-order accurate in time for the logarithmic free energy.

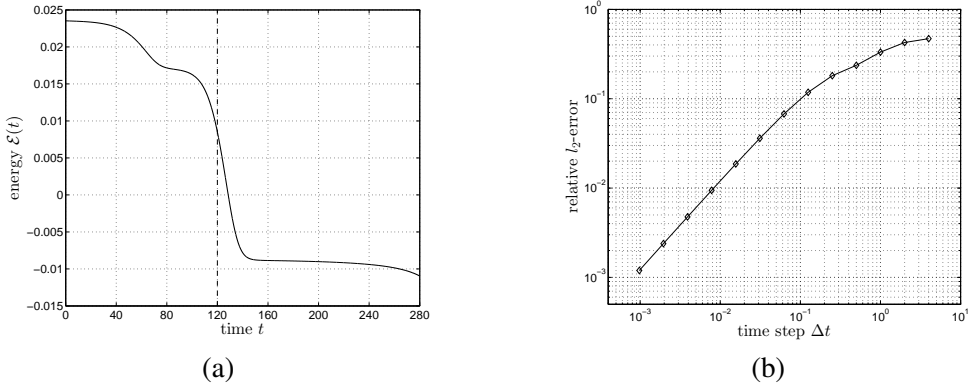
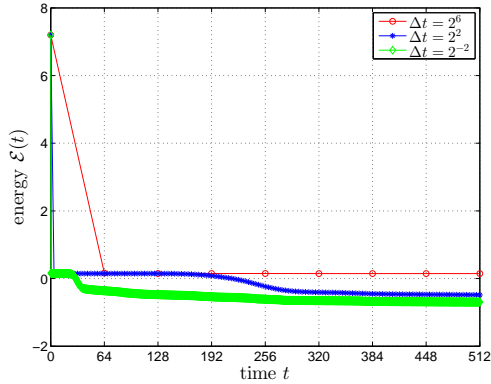
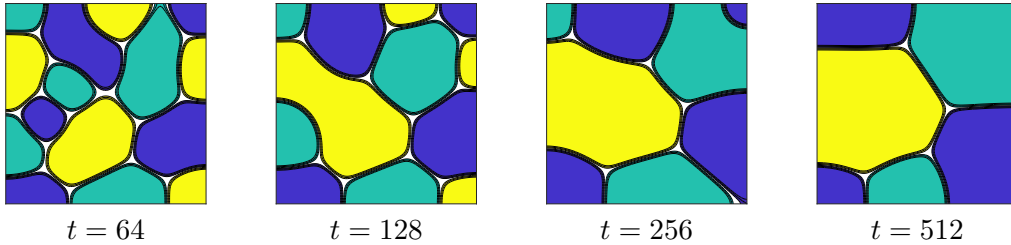


FIGURE 10. (a) Evolution of $\mathcal{E}(t)$ for the reference solution with $\theta = 0.3$, $\theta_c = 1$, $\epsilon = 0.25$, $h = 2\pi/128$. (b) Relative l_2 -errors of $c(x, 120)$ for various time steps.

5.2. Energy stability of the proposed scheme. In order to investigate the energy stability for the logarithmic free energy, we take the initial conditions as

$$\begin{aligned} c_1(x, y, 0) &= \frac{1}{3} + \text{rand}(x, y), & c_2(x, y, 0) &= \frac{1}{3} + \text{rand}(x, y), \\ c_3(x, y, 0) &= 1 - c_1(x, y, 0) - c_2(x, y, 0) \end{aligned}$$

on $\Omega = [0, 2\pi] \times [0, 2\pi]$. Here, $\text{rand}(x, y)$ is a random number between -0.1 and 0.1 , and we use $\theta = 0.3$, $\theta_c = 1$, $\epsilon = 0.1$, $h = 2\pi/128$, and $\text{tol} = 10^{-6}$. Figure 11 shows the evolution of $\mathcal{E}(t)$ with different time steps. All the energy curves are also nonincreasing in time for the logarithmic free energy. Figure 12 shows the evolution of $c(x, y, t)$ with $\Delta t = 2^{-2}$.

FIGURE 11. Evolution of $\mathcal{E}(t)$ with different time steps.FIGURE 12. Evolution of $c(x, y, t)$ with $\theta = 0.3$, $\theta_c = 1$, $\epsilon = 0.1$, $h = 2\pi/128$, and $\Delta t = 2^{-2}$. In each snapshots, the yellow, green, and blue regions indicate c_1 , c_2 , and c_3 , respectively, and contour lines represent $c_i = 0.45, 0.5$, and 0.55 .

6. CONCLUSIONS

In this paper, we proposed the cCS scheme for the vCH equation and proved its unconditional energy stability. For the polynomial free energy and linear convex splitting, we confirmed that the scheme is first-order accurate in time and unconditionally energy stable. Owing to the linear convex splitting, we solved the vCH equation efficiently (the CPU time was almost linear with respect to the number of components N). For the logarithmic free energy and nonlinear convex splitting, we showed the robustness of the nonlinear solver and the necessity of the preconditioner. And we also demonstrated that the scheme is first-order accurate in time and unconditionally energy stable.

We note that order of time accuracy of the cCS scheme can be improved by various approaches. One of them is to combine with an s -stage implicit–explicit Runge–Kutta method [1, 29, 30] and extension of the cCS scheme to high-order time accuracy can be considered as the scope of future study.

REFERENCES

- [1] U.M. Ascher, S.J. Ruuth, and R.J. Spiteri, *Implicit–explicit Runge–Kutta methods for time-dependent partial differential equations*, Appl. Numer. Math. **25** (1997), 151–167.
- [2] V.E. Badalassi, H.D. Ceniceros, and S. Banerjee, *Computation of multiphase systems with phase field models*, J. Comput. Phys. **190** (2003), 371–397.
- [3] J.W. Barrett and J.F. Blowey, *An error bound for the finite element approximation of the Cahn–Hilliard equation with logarithmic free energy*, Numer. Math. **72** (1995), 1–20.
- [4] J.W. Barrett and J.F. Blowey, *An error bound for the finite element approximation of a model for phase separation of a multi-component alloy*, IMA J. Numer. Anal. **16** (1996), 257–287.
- [5] J.F. Blowey, M.I.M. Copetti, and C.M. Elliott, *Numerical analysis of a model for phase separation of a multicomponent alloy*, IMA J. Numer. Anal. **16** (1996), 111–139.
- [6] F. Boyer and C. Lapuerta, *Study of a three component Cahn–Hilliard flow model*, ESAIM: M2AN **40** (2006), 653–687.
- [7] F. Boyer and S. Minjeaud, *Hierarchy of consistent n-component Cahn–Hilliard systems*, Math. Models Meth. Appl. Sci. **24** (2014), 2885–2928.
- [8] J.W. Cahn and J.E. Hilliard, *Free energy of a nonuniform system. I. Interfacial free energy*, J. Chem. Phys. **28** (1958), 258–267.
- [9] L.-Q. Chen, *Phase-field models for microstructure evolution*, Annu. Rev. Mater. Res. **32** (2000), 113–140.
- [10] J.P. Desi, H.H. Edrees, J.J. Price, E. Sander, and T. Wanner, *The dynamics of nucleation in stochastic Cahn–Morrall systems*, SIAM J. Appl. Dyn. Syst. **10** (2011), 707–743.
- [11] S. Dong, *An efficient algorithm for incompressible N-phase flows*, J. Comput. Phys. **276** (2014), 691–728.
- [12] C.M. Elliott and S. Luckhaus, *A generalised diffusion equation for phase separation of a multi-component mixture with interfacial free energy*, IMA Preprint Series 887, 1991.
- [13] C.M. Elliott and A.M. Stuart, *The global dynamics of discrete semilinear parabolic equations*, SIAM J. Numer. Anal. **30** (1993), 1622–1663.
- [14] D.J. Eyre, *Unconditionally gradient stable time marching the Cahn–Hilliard equation*, MRS Proc. **529** (1998), 39–46.
- [15] D. de Fontaine, *A computer simulation of the evolution of coherent composition variations in solid solutions*, Ph.D. Thesis, Northwestern University, 1967.
- [16] H. Garcke, B. Nestler, and B. Stoth, *On anisotropic order parameter models for multi-phase systems and their sharp interface limits*, Phys. D **115** (1998), 87–108.
- [17] Z. Guan, C. Wang, and S.M. Wise, *A convergent convex splitting scheme for the periodic nonlocal Cahn–Hilliard equation*, Numer. Math. **128** (2014), 377–406.
- [18] D. Jeong and J. Kim, *A practical numerical scheme for the ternary Cahn–Hilliard system with a logarithmic free energy*, Phys. A **442** (2016), 510–522.
- [19] D. Jeong and J. Kim, *Practical estimation of a splitting parameter for a spectral method for the ternary Cahn–Hilliard system with a logarithmic free energy*, Math. Meth. Appl. Sci. **40** (2017), 1734–1745.
- [20] J. Kim, K. Kang, and J. Lowengrub, *Conservative multigrid methods for ternary Cahn–Hilliard systems*, Comm. Math. Sci. **2** (2004), 53–77.
- [21] H.G. Lee, J.-W. Choi, and J. Kim, *A practically unconditionally gradient stable scheme for the N-component Cahn–Hilliard system*, Phys. A **391** (2012), 1009–1019.
- [22] H.G. Lee and J. Kim, *A second-order accurate non-linear difference scheme for the N-component Cahn–Hilliard system*, Phys. A **387** (2008), 4787–4799.
- [23] H.G. Lee and J. Kim, *An efficient and accurate numerical algorithm for the vector-valued Allen–Cahn equations*, Comput. Phys. Commun. **183** (2012), 2107–2115.
- [24] H.G. Lee, J. Shin, and J.-Y. Lee, *First- and second-order energy stable methods for the modified phase field crystal equation*, Comput. Methods Appl. Mech. Engrg. **321** (2017), 1–17.
- [25] J.E. Morral and J.W. Cahn, *Spinodal decomposition in ternary systems*, Acta Metall. **19** (1971), 1037–1045.

- [26] B. Nestler and A.A. Wheeler, *A multi-phase-field model of eutectic and peritectic alloys: numerical simulation of growth structures*, Phys. D **138** (2000), 114–133.
- [27] É. Oudet, *Approximation of partitions of least perimeter by Γ -convergence: around Kelvin’s conjecture*, Exp. Math. **20** (2011), 260–270.
- [28] J. Shin, H.G. Lee, and J.-Y. Lee, *First and second order numerical methods based on a new convex splitting for phase-field crystal equation*, J. Comput. Phys. **327** (2016), 519–542.
- [29] J. Shin, H.G. Lee, and J.-Y. Lee, *Convex Splitting Runge–Kutta methods for phase-field models*, Comput. Math. Appl. **73** (2017), 2388–2403.
- [30] J. Shin, H.G. Lee, and J.-Y. Lee, *Unconditionally stable methods for gradient flow using Convex Splitting Runge–Kutta scheme*, J. Comput. Phys. **347** (2017), 367–381.
- [31] R. Tavakoli, *Computationally efficient approach for the minimization of volume constrained vector-valued Ginzburg–Landau energy functional*, J. Comput. Phys. **295** (2015), 355–378.
- [32] R. Tavakoli, *Unconditionally energy stable time stepping scheme for Cahn–Morral equation: Application to multi-component spinodal decomposition and optimal space tiling*, J. Comput. Phys. **304** (2016), 441–464.
- [33] G.I. Tóth, T. Pusztai, and L. Gránásy, *Consistent multiphase-field theory for interface driven multidomain dynamics*, Phys. Rev. B **92** (2015), 184105.
- [34] G.I. Tóth, M. Zarifi, and B. Kvamme, *Phase-field theory of multicomponent incompressible Cahn–Hilliard liquids*, Phys. Rev. E **93** (2016), 013126.
- [35] L. Vanherpe, F. Wendler, B. Nestler, and S. Vandewalle, *A multigrid solver for phase field simulation of microstructure evolution*, Math. Comput. Simul. **80** (2010), 1438–1448.
- [36] C. Wang, X. Wang, and S.M. Wise, *Unconditionally stable schemes for equations of thin film epitaxy*, Discrete Cont. Dyn. S. **28** (2010), 405–423.
- [37] C. Wang and S.M. Wise, *An energy stable and convergent finite-difference scheme for the modified phase field crystal equation*, SIAM J. Numer. Anal. **49** (2011), 945–969.
- [38] S.M. Wise, C. Wang, and J.S. Lowengrub, *An energy-stable and convergent finite-difference scheme for the phase field crystal equation*, SIAM J. Numer. Anal. **47** (2009), 2269–2288.